Towards low-carbon deep soil mixing: alkali activation of fly ash and slags

Deepesh Bansal[1], *Shuxiang* Zhang[1], *Ziyu* Lu[1], *Deepak* Patwa[1], and *Kai* Yao[1,2*]

[1] School of Qilu Transportation, Shandong University, Jinan-250002, China
[2] Xinjiang Research Institute of Shandong University, Changji-831100, China

Abstract. Deep Soil Mixing (DSM) is widely used to improve soft and problematic soils, traditionally relying on cement or lime as binders. However, their high carbon footprint and durability limitations under aggressive environments highlight the need for sustainable alternatives. This study evaluates alkali-activated binders produced from industrial byproducts: fly ash (FA), granulated blast furnace slag (GBFS), and calcium carbide slag (CCS), for stabilizing silty clay. Sodium hydroxide (NH) and sodium silicate (SS) were used as the primary activators, while red mud was incorporated as a minor supplementary alkaline additive. Binder slurries were prepared with a fixed Na_2O content of 8% and an NH/SS ratio of 1.5, while the water-to-binder ratio was varied from 0.6 to 1.2. Slurry workability was characterized using a Marsh funnel test, and the mechanical performance of stabilized soils was evaluated through unconfined compressive strength tests after 7 and 28 days of curing. Results show that FA-rich mixtures exhibit limited early strength, whereas higher GBFS and CCS contents promote C-A-S-H gel formation, matrix densification, and significantly enhanced strength. An optimal FA:GBFS:CCS ratio of 2:5:3 achieved favorable slurry properties and delivered 20–30% higher strength than cement-stabilized soil, demonstrating the potential of this low-carbon binder for sustainable DSM practice.

1 Introduction

Rapid urban growth in Jinan, Shandong Province, particularly the construction of metro networks and tall building foundations, has intensified the demand for deep foundation solutions for construction activities on weak and heterogeneous soils [1, 2]. Among the available ground-improvement approaches, Deep Soil Mixing (DSM) has become a widely adopted technique, as it strengthens in-situ soils through mechanical blending with cementitious or chemical binders while offering advantages such as low vibration, limited excavation requirements, suitability for constrained urban sites, and flexibility in layered ground conditions [3-5].

Conventional DSM practices predominantly rely on lime and cement binders due to their availability and rapid strength gain, with performance linked to hydration, ion exchange, and pozzolanic reactions [6-8]. However, these binders raise growing environmental and technical concerns. Cement manufacture produces approximately 0.8–0.9 tonnes of CO_2 per tonne of product, while lime generates around 0.7–0.75 tonnes, together contributing to roughly 7–10% of global anthropogenic CO_2 emissions [9-11]. Additional drawbacks include shrinkage at early ages [12], curing sensitivity [13], and deterioration risks in sulfate-rich or acidic environments [14]. These issues have motivated increasing interest in low-carbon binder systems, particularly alkali-activated binders (AABs).

AABs have gained increasing attention as viable substitutes for conventional cement, owing to their capacity to incorporate industrial byproducts while delivering mechanical strength and durability performance comparable to (or in some cases surpassing) traditional binders, alongside markedly reduced CO_2 emissions [15, 16]. These systems are generally produced by chemically activating aluminosilicate-rich precursors, such as fly ash (FA) or ground-granulated blast furnace slag (GBFS), with alkaline solutions or solid activators [16-18]. Common activators employed in AABs are sodium hydroxide (NH), sodium silicate (SS), sodium carbonate (NC), and calcium hydroxide (CH), each exhibiting distinct dissolution behaviors and reaction kinetics that influence binder development [15].

Despite encouraging findings in the stabilization of concrete and shallow soil stabilization [19-21], the application of AAB systems in DSM remains comparatively underexplored. The effective integration of AABs into DSM requires the coordinated optimization of material composition (precursor selection, ratios, and activator chemistry) and field implementation parameters (binder dosage, water–to–binder ratio (W/B), and slurry characteristics) [15-17]. These coupled factors govern the development of gels, their strength evolution, durability, and constructability.

This study aims to develop a low-carbon, high-performance alkali-activated binder system designed explicitly for the DSM treatment of problematic silty

* Corresponding author: yaokai@sdu.edu.cn

clays in Jinan. A multi-waste precursor system comprising FA, GBFS, and calcium carbide slag (CCS) was investigated to enhance soil strength and overall engineering behavior. Sodium hydroxide and sodium silicate served as the primary alkaline activators because these activators provide, respectively, a highly alkaline environment for precursor dissolution and soluble silicate species that support gel formation in the FA–GBFS–CCS system [37]. This choice is particularly suitable for the present precursor blend because the fly ash is a low-calcium Class F material, whereas GBFS and CCS already supply calcium within the binder system. Additionally, Red mud (RM) was incorporated only as a minor supplementary alkaline additive under the fixed activator regime. Owing to its inherent alkalinity and reactive oxides, RM can serve as an auxiliary activator or precursor; however, its content must be carefully optimized to avoid adverse effects [22]. This research supports the strategic goals of China's 15th Five-Year Plan, which prioritize the sustainable, high-value utilization of bulk industrial solid waste and advance greener, more resilient DSM technologies.

2 Materials and methodology

2.1 Materials

A locally sourced soil obtained from the Yellow River floodplain in Jinan, Shandong Province (China), was used as the base material. FA, GBFS, and CCS were obtained from a nearby thermal power plant, a titanium dioxide production facility, and a local supplier, respectively. Ordinary Portland Cement (OPC, 42.5 grade) was included as a reference binder to benchmark the soil–AAB mixtures against conventional cement-stabilized soil.

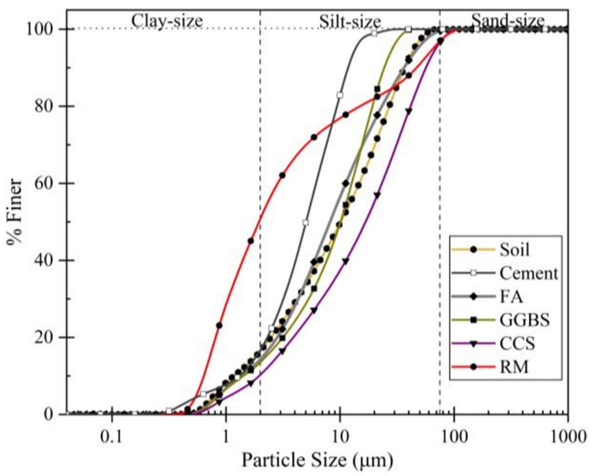

Fig. 1. Particle size distribution curves of different materials.

The particle size distributions of the soil, FA, GBFS, CCS, RM, and OPC were determined using a Microtrac S3500 laser particle size analyzer, and the gradation curves are presented in Fig. 1. The soil has a liquid limit of approximately 35% and a plasticity index of 18.1%, which classifies it as having low to medium plasticity clay according to the Unified Soil Classification System (USCS).

Representative scanning electron microscopy (SEM) images of the raw materials are shown in Fig. 2. The soil, GBFS, CCS, RM, and OPC primarily consist of irregular angular particles, whereas FA exhibits predominantly spherical particles, as typically observed in pulverized coal combustion ash.

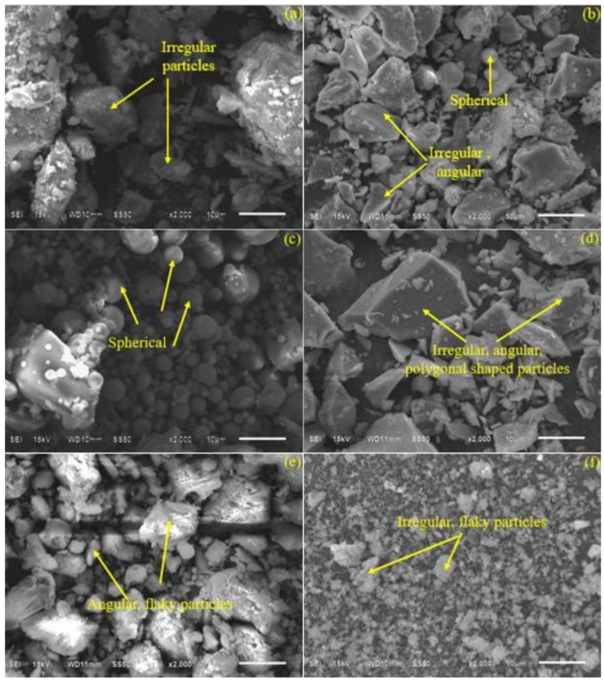

Fig. 2. SEM images: (a) Soil, (b) Cement, (c) FA, (d) GBFS, (e) CCS, (f) RM.

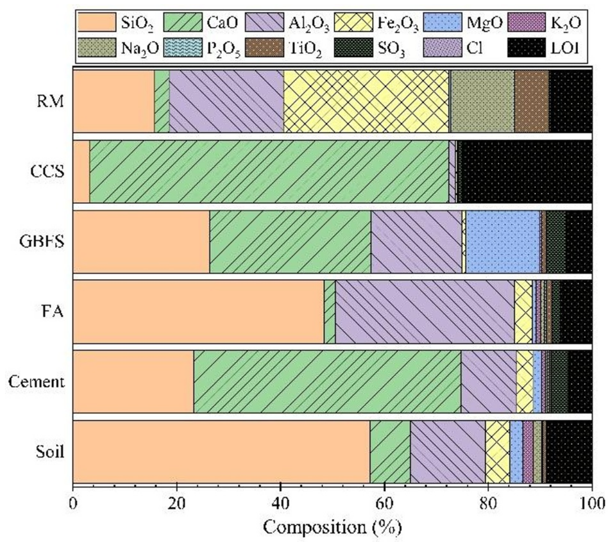

Fig. 3. Chemical composition of different materials.

Chemical oxide compositions obtained through X-ray fluorescence (XRF) are shown in Fig. 3. Based on ASTM C618 [23], the FA used in this study is categorized as Class F, as indicated by its low CaO content (2.14%). The relatively high SiO_2 and Al_2O_3 contents in FA and GBFS ensure adequate aluminosilicate availability for alkali activation, while the elevated CaO contents in GBFS and CCS provide calcium necessary for hydration and gel formation.

Alkali activation was achieved using SS, NH, and RM. The NH pellets (96% purity) and SS solution (SiO_2/Na_2O modulus = 3.3, 63% water content) were obtained from local suppliers. RM was sourced from a bauxite refining facility in Zibo City, Shandong Province, and its chemical composition is documented, along with that of the other materials, in Fig. 3. Owing to its high alkalinity and significant Al_2O_3 and Fe_2O_3 contents, RM was incorporated as a minor supplementary alkaline additive. In the present mix design, RM dosage was fixed at 5% of the activator dosage, corresponding to 1.79 g per kg of dry soil. Fig. 4 shows the different materials used in this study.

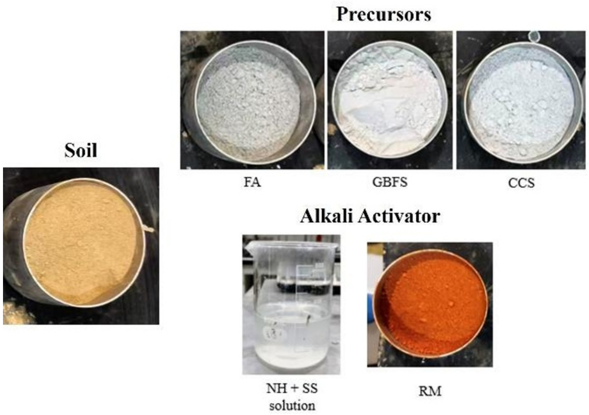

Fig. 4. Different materials used in the study.

2.2 Methodology

All soil samples and binder precursors were oven-dried and subsequently sealed in airtight containers prior to testing. For the reference OPC system, predetermined quantities of OPC and water were mixed in a Hobart mixer for approximately 10 minutes to obtain a slurry for rheological measurements. Soil–OPC blends were prepared in the same mixer by combining soil, OPC, and water according to the specified water content, binder dosage, and water-to-binder ratio.

For alkali-activated binder mixtures, the activator was prepared by first dissolving NH pellets in the required portion of water, after which the SS solution was added to achieve the desired composition. Only the additional water not already present in the SS solution was used to dissolve NH, thereby maintaining the target W/B ratio. The prepared activator was stored in a curing chamber at 20 ± 2 °C and 95% RH for about 24 h before use. This conditioning period is essential for silicate-based activators because silicate species undergo time-dependent structural rearrangement that is highly influenced by concentration and temperature. Allowing the activator to equilibrate promotes a more stable silicate distribution and temperature, resulting in improved consistency in precursor dissolution, rheological behavior, and early-age strength development [20, 24].

In case of slurry-related studies, dried precursors (FA, GBFS, CCS) were manually blended for 1–2 minutes to ensure uniformity, followed by the addition of red mud and the prepared activator. Mixing was then continued for 10 min in a Hobart mixer. Soil–AAB mixtures were prepared using the same procedure, combining soil, water, precursors, and activator, and then mixing for 10 minutes prior to specimen casting.

Marsh funnel viscosity [25], bleeding [26], and pH [27] of binder slurry were measured. In the case of soil-binder mix, strength evaluation was carried out using unconfined compressive strength (UCS) testing. Cylindrical specimens with dimensions of 50 mm in diameter and 100 mm in height were molded in split cylinders, cured at 20 ± 2 °C and 95% relative humidity, demolded after 24 h, and subsequently tested at curing ages of 7 and 28 days. The UCS tests were conducted at a loading rate of 1 mm/min. Additionally, SEM was performed on selected hardened soil–binder samples after UCS testing at the corresponding age (7 or 28 days) to investigate the microstructural basis of strength development, including gel formation, matrix densification, visible porosity, and partially reacted particles.

2.3 Design of experiments

An initial parametric investigation was conducted to determine an appropriate water-to-binder ratio for alkali-activated slurry preparation, varying W/B from 0.6 to 1.2. This preliminary screening was conducted only on the OPC reference system and AAB4. The latter was selected as a representative alkali-activated formulation with a balanced FA–GBFS–CCS composition, avoiding an extreme ternary blend. Based on the resulting slurry workability and strength performance, W/B = 0.8 was selected for subsequent testing. Thereafter, seven representative precursor formulations from the FA–GBFS–CCS ternary blend system were selected for detailed evaluation, as presented in Table 1. These mixtures were designed to cover FA-rich, GBFS-dominant, CCS-enhanced, and relatively balanced regions of the mixture domain, thereby enabling a structured assessment of composition-dependent trends relevant to DSM applications.

The experimental design aimed to: (i) examine how variations in calcium availability and reactive silica/alumina content influence alkali-activation reactions and gel development; (ii) ensure sufficient flowability and practical suitability under DSM conditions; and (iii) maintain a sufficiently focused experimental matrix to permit clear interpretation of precursor-composition effects. Because the FA–GBFS–CCS system is a constrained ternary mixture in which the component proportions sum to 100%, the mixture space is reduced to two independent variables. Following Cornell's [28] guidance for mixture experiments, a limited but representative set of formulations can be used to capture the principal compositional trends without excessive experimental complexity. Accordingly, the present study was designed as a focused comparison of representative blended precursor compositions rather than a full screening of all single-, binary-, and ternary-component end members.

Table 1. Different combinations of precursors for the study.

ID	FA (%)	GBFS (%)	CCS (%)
AAB1	50	30	20
AAB2	40	40	20
AAB3	40	30	30
AAB4	30	50	20
AAB5	30	40	30
AAB6	20	50	30
AAB7	25	35	40

Throughout this testing, activator chemistry was kept constant to isolate the effect of precursor composition. A fixed SS/NH of 1.5 was adopted, in line with literature suggesting optimal Si/Al ratios are achieved for SS/NH values of 1–2 for enhanced strength and matrix density in alkali-activated systems [16, 29]. The Na_2O dosage was maintained at 8%, corresponding to 16 g Na2O per 1 kg of dry soil in the present mix design. Under this condition, the corresponding activator components were 14.35 g NH and 21.53 g SS per kg of dry soil. RM was added as a minor supplementary alkaline additive at 5% of the activator dosage [30, 31].

A precursor dosage of 20% by dry weight of soil was selected to reflect a mid-range treatment level commonly applied in DSM projects, which typically span from 10% to 30% depending on performance requirements [6, 16, 32]. Here, this dosage refers to the FA–GBFS–CCS precursor blend reported in Table 1. For controlled laboratory specimen preparation, the oven-dried soil was reconstituted to an initial water content equal to 1.2 times its liquid limit (42%). This prescribed value was selected to represent a weak, high-moisture condition relevant to wet DSM and to ensure consistent comparison among mixtures; it was not intended to reproduce a specific in-situ field moisture content.

3 Results and discussion

3.1 Variation of W/B

Preliminary trials were conducted using OPC and an AAB4, with water-to-binder ratios ranging from 0.6 to 1.2. Table 2 summarizes the fresh and hardened properties of the resulting slurries, including Marsh funnel viscosity and UCS at 28 days.

Although no formal standards define viscosity thresholds for DSM applications, several industry guidelines and international standards suggest that acceptable Marsh funnel viscosities range from 30 to 70 sec/qt to ensure adequate pumpability, injection stability, and uniform soil penetration [33-35]. In line with federal performance recommendations, a minimum 28-day UCS of 1 MPa was targeted for the soil–binder mixtures [32, 36]. Among the tested formulations, the OPC-based mixes at W/B ratios of 0.7–0.8 met both the strength and viscosity criteria. However, the AAB4 system achieved an optimum viscosity of 58.8 sec/qt and a UCS of 1.20 MPa at a W/B of 0.8 only.

At lower W/B ratios (0.6), AAB4 slurries exhibited significantly elevated viscosities, rendering them unsuitable for field injection. Conversely, W/B ratios ≥1.0 resulted in lower viscosities but compromised strength, with UCS values falling below the 1 MPa threshold for both binder systems. The steeper drop in UCS beyond a W/B ratio of 1.0 may suggest that binder dilution effects outweigh any benefit of additional water for precursor dissolution and subsequent gel formation in the alkali-activated system, as well as cement hydration in the OPC system.

Yu et al. [24] also reported that increasing the W/B ratio from 0.6 to 1.2 in cement-stabilized marine clay led to a progressive reduction in UCS and a substantial increase in workability. The results emphasized a similar trade-off between pumpability and mechanical performance, validating the selection of W/B = 0.8 as an effective compromise for wet DSM operations.

Based on these trends, a W/B ratio of 0.8 was selected for subsequent testing. This ratio offers a practical balance between fresh state workability and hardened strength performance, supporting both binder dispersion and in-situ soil treatment efficiency. Notably, while total moisture includes both slurry and native soil water, W/B calculations in this study only accounted for slurry water to maintain consistency across mix designs.

Table 2. Preliminary trials of binders for different W/B.

W/B	OPC		AAB4	
	Viscosity (sec/qt)	UCS-28 d (MPa)	Viscosity (sec/qt)	UCS-28 d (MPa)
0.6	80.0 ± 0.8	NP	214 ± 1.3	NP
0.7	37.0 ± 0.6	1.59 ± 0.02	98.2 ± 0.6	NP
0.8	33.0 ± 0.5	1.37 ± 0.01	58.8 ± 0.3	1.20 ± 0.01
1.0	28.6 ± 0.7	1.04 ± 0.03	40.5 ± 0.7	0.86 ± 0.05
1.2	27.2 ± 0.3	0.83 ± 0.04	34.6 ± 0.3	0.65 ± 0.07

NP: Not Performed

3.2 Variation of the precursors proportion

The performance of the alkali-activated binder systems was assessed through seven precursor combinations (AAB1–AAB7). The slurry properties, including viscosity, bleeding/sedimentation, and pH, are presented in Table 3, while the 7-day and 28-day UCS results are shown in Fig. 5.

As shown in Table 3, all AAB slurries exhibited stable rheological behavior, with Marsh funnel viscosities ranging from 50.4 to 68.4 sec/qt and no observable bleeding or sedimentation. The consistently high pH values (13.40–13.50) indicate a strongly alkaline environment, favorable for the dissolution of aluminosilicate precursors and subsequent gel formation. In contrast, the OPC slurry showed a markedly lower viscosity (33.0 sec/qt), a lower pH (12.8), and measurable sedimentation of 3.2% after 15 minutes, reflecting inferior slurry stability. The absence of bleeding in all AAB mixes highlights their suitability for DSM applications, where segregation resistance is critical.

Table 3. Slurry properties for different binders.

Sample	Viscosity (sec/qt)	Bleeding/ Sedimentation (%)	pH
AAB1	54.6 ± 0.6	0	13.40 ± 0.02
AAB2	50.4 ± 0.4	0	13.50 ± 0.02
AAB3	57.4 ± 0.5	0	13.40 ± 0.03
AAB4	58.8 ± 0.4	0	13.45 ± 0.02
AAB5	63.0 ± 0.3	0	13.40 ± 0.03
AAB6	58.8 ± 0.4	0	13.50 ± 0.01
AAB7	68.4 ± 0.5	0	13.45 ± 0.02
OPC	33.0 ± 0.3	3.20	12.80 ± 0.05

The UCS results in Fig. 5 demonstrate a pronounced dependence of strength development on precursor chemistry. Across the AAB formulations, increasing the proportion of GBFS and CCS resulted in substantial improvements in both early-age and long-term strength. This trend reflects the higher calcium availability and greater intrinsic reactivity of GBFS and CCS under alkaline activation, which promote the formation of calcium-rich binding gels, mainly C–A–S–H-type phases. These reaction products strengthen the treated soil by binding soil particles and residual precursor grains, filling pore spaces, and forming a denser, more continuous matrix, thereby increasing resistance to axial compression.

Among all mixes, AAB6 (50% GBFS and 30% CCS) achieved the highest 28-day UCS of 1.70 MPa, while maintaining a practical viscosity of 58.8 sec/qt. In contrast, AAB1, characterized by a high FA content (50% FA), exhibited the lowest UCS of 0.53 MPa, despite having a comparable viscosity (54.6 sec/qt). This represents an approximately 220% increase in UCS from AAB1 to AAB6, underscoring the critical role of calcium-rich precursors in promoting the formation of a denser load-bearing binder matrix. Across all AAB mixes, the UCS increased by approximately 61–77% between 7 and 28 days, indicating continued reaction and progressive densification of the binder matrix. These delayed strength gains are consistent with continued alkali-activation reactions, progressive gel formation, and matrix densification in the alkali-activated systems.

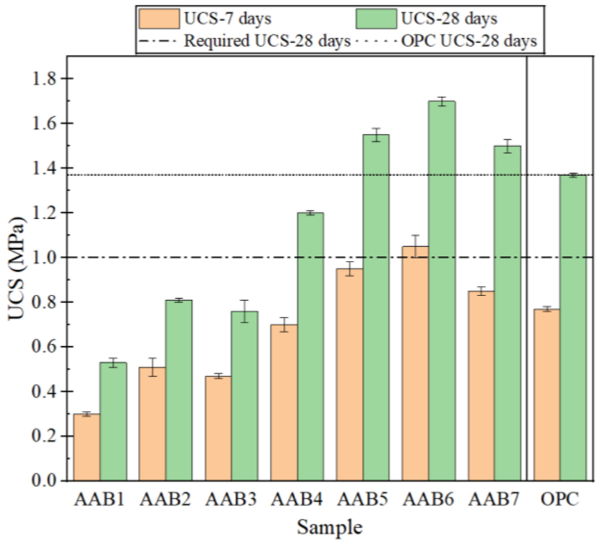

Fig. 5. UCS of soil-binder mixes.

When compared with OPC, AAB5–AAB7 demonstrated superior mechanical performance at both curing ages. Specifically, the UCS values of these AAB formulations were 23–37% higher at 7 days and 13–24% higher at 28 days than those of OPC. These results highlight the enhanced reactivity and sustained strength development of optimized alkali-activated binders relative to conventional cement-based systems.

The suitability of binder systems for DSM applications was evaluated against two commonly adopted criteria: a minimum 28-day UCS of 1.0 MPa [32, 36] and a Marsh funnel viscosity of 30-70 sec/qt [33-35]. Based on these thresholds, AAB4–AAB7 satisfied both strength and workability requirements, with AAB6 emerging as the most promising formulation due to its optimal balance of rheology and strength. In contrast, AAB1–AAB3 failed to meet the UCS requirement despite having acceptable viscosities, highlighting the need for sufficient calcium content in the precursor blend.

The mechanical trends observed are strongly supported by the SEM observations shown in Fig. 6. The OPC specimens (Fig. 6a and 6b) exhibit a heterogeneous microstructure with visible capillary pores and needle-like ettringite crystals, particularly at early ages. The strength development at 28 days for the OPC-based mix is primarily governed by the formation of a conventional C–S–H gel. In contrast, AAB6 exhibits a significantly denser, more homogeneous matrix, characterized by the formation of a C–A–S–H gel upon alkali activation of GBFS and CCS (Fig. 6d).

At 7 days (Fig. 6c), partially reacted GBFS particles are embedded within a developing C–A–S–H gel network, while at 28 days (Fig. 6d), the microstructure evolves into a compact, continuous gel matrix with minimal visible porosity. Conversely, FA-dominant systems, such as AAB3 (Fig. 6e), exhibit incomplete gel formation, residual unreacted particles, and a more porous microstructure, which explains their comparatively lower UCS. These microstructural differences confirm that GBFS- and CCS-rich systems promote denser, more cohesive reaction products, which directly translate into improved mechanical performance.

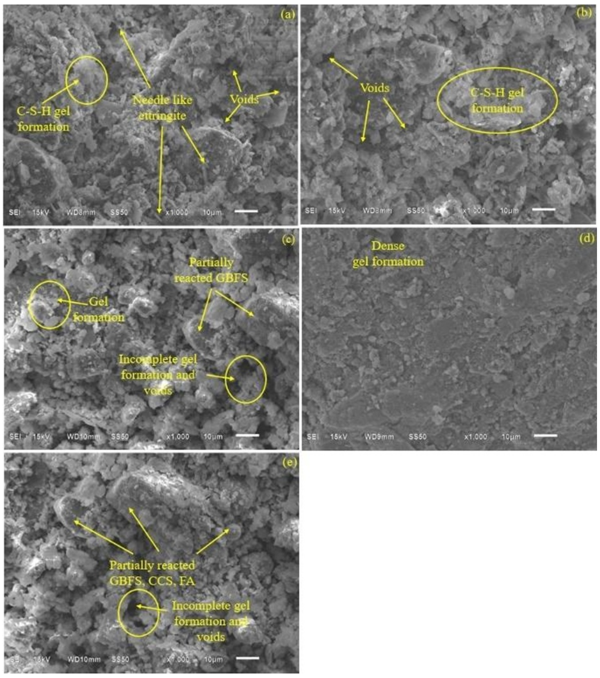

Fig. 6. SEM images of selected hardened soil–binder specimens after UCS at the indicated age: (a) OPC-7 days, (b) OPC-28 days, (c) AAB6-7 days, (d) AAB6-28 days, (e) AAB3-28 days.

4 Conclusions

This study investigated the fresh and hardened performance of alkali-activated binders formulated with FA, GBFS, and CCS for application in wet DSM, with particular emphasis on the effects of water-to-binder ratio and precursor composition. Based on the experimental results, the following conclusions can be drawn:

- The W/B ratio strongly governs slurry workability and strength development; a value of 0.8 provides the optimal balance for wet DSM, satisfying both viscosity and UCS requirements for alkali-activated binders.
- All AAB slurries exhibited stable fresh-state behavior, with Marsh funnel viscosities of 50–68 sec/qt, no bleeding or sedimentation, and high alkalinity, outperforming OPC in terms of slurry stability.
- Strength development was highly dependent on precursor composition, with increasing GBFS and CCS contents markedly enhancing both early-age and 28-day UCS due to improved calcium availability and reactivity.
- The optimized formulation AAB6 (50% GBFS + 30% CCS) achieved the highest 28-day UCS (1.70 MPa) while maintaining suitable workability, exceeding OPC performance at both 7 and 28 days.
- SEM observations confirmed that GBFS- and CCS-rich systems form denser, more homogeneous gel matrices, whereas FA-dominant mixes exhibit incomplete reaction and porous microstructures.

This study proposes a novel binder system that incorporates secondary materials as a sustainable, durable alternative to conventional cement for deep soil mixing applications. The findings establish a valuable reference for the development of low-carbon soil stabilization technologies in soft ground engineering. Future investigations should place greater focus on the role of activator characteristics in governing binder performance. In addition, a systematic assessment of the residual, unreacted binder is needed to quantify reaction efficiency better and support the design of optimized mixtures for soils with different initial water contents. Further evaluation of long-term durability, shear strength, and sustainability indicators is crucial to fully understand the behavior of the binder and verify its applicability in practical engineering scenarios.

This research work is supported by Regional Collaborative Innovation Program of Changji Hui Autonomous Prefecture (2025X02), and Jinan Science and Technology Bureau Project (202333051).

All data supporting the findings of this work will be made available upon request.

Deepesh Bansal: Conceptualization, Methodology, Investigation, Formal analysis, Writing – original draft. Shuxiang Zihan and Ziyu Lu: Investigation, Formal analysis. Deepak Patwa: Methodology, Writing – review and editing. Kai Yao: Supervision, Writing – review and editing.

References

1. Z. Liu, X. Ma, D. Zhou, L. Lu, H. Zhang, Y. Bai, H. Han, The geological origins and soil properties of loess-like silty clay: A case study in the Jinan area, Sci. Rep. **14**, 1–12 (2024). https://doi.org/10.1038/s41598-024-63394-0
2. G.F. Wang, Y.X. Wu, L. Lu, G. Li, J.S. Shen, Investigation of the geological and hydrogeological environment with relation to metro system construction in Jinan, China, Bull. Eng. Geol. Environ. **78**, 1005–1024 (2019). https://doi.org/10.1007/s10064-017-1140-2
3. B. Abdelmalek, K.P. Soon, C. Gary, Strength Properties of Cement Treated Coode Island Silt by the Soil Mixing Method, in: Geotech. Eng. Transp. Proj., pp. 1421–1428 (2012). https://doi.org/doi:10.1061/40744(154)132
4. A. Porbaha, State of the art in deep mixing technology. Part I: Basic concepts and overview, Gr. Improv. **2,** 81–92 (1998). https://doi.org/10.1680/grim.2000.4.3.111
5. M.J. Singh, K. Yao, T. Lei, S. Liu, Y. Zhang, Z. Yao, M. Beer, Load-bearing performance and failure behavior of multi-flange deep cement mixing columns, Mar. Georesources Geotechnol. 1–15 (2025). https://doi.org/10.1080/1064119X.2025.2538816
6. S. Horpibulsk, R. Rachan, A. Suddeepong, A. Chinkulkijniwat, Strength development in cement admixed Bangkok clay: Laboratory and field investigations, Soils Found. **51**, 239–251 (2011). https://doi.org/10.3208/sandf.51.239
7. P. Jamsawang, N. Nuansrithong, P. Voottipruex, S. Songpiriyakij, P. Jongpradist, Laboratory investigations on the swelling behavior of composite expansive clays stabilized with shallow and deep clay-cement mixing methods, Appl. Clay Sci. **148**, 83–94 (2017). https://doi.org/10.1016/j.clay.2017.08.013

8. P. Van Ngoc, B. Turner, J. Huang, R. Kelly, Long-term strength of soil-cement columns in coastal areas, Soils Found. 57, 645–654 (2017). https://doi.org/10.1016/j.sandf.2017.04.005
9. P. Sargent, The development of alkali-activated mixtures for soil stabilisation, Woodhead Publishing Limited, (2015). https://doi.org/10.1533/9781782422884.4.555
10. M. Zhang, H. Guo, T. El-Korchi, G. Zhang, M. Tao, Experimental feasibility study of geopolymer as the next-generation soil stabilizer, Constr. Build. Mater. **47**, 1468–1478 (2013). https://doi.org/10.1016/j.conbuildmat.2013.06.017
11. B.C. McLellan, R.P. Williams, J. Lay, A. van Riessen, G.D. Corder, Costs and carbon emissions for geopolymer pastes in comparison to ordinary portland cement, J. Clean. Prod. **19**, 1080–1090 (2011). https://doi.org/10.1016/j.jclepro.2011.02.010
12. K. Sobhan, J. Ramirez, D. Reddy, Cement stabilization of highly organic subgrade soils to control secondary compression settlement, Transp. Res. Rec. 103–112 (2012). https://doi.org/10.3141/2310-11
13. T.O. Ho, W.B. Chen, J.H. Yin, P.C. Wu, D.C.W. Tsang, Stress-Strain behaviour of Cement-Stabilized Hong Kong marine deposits, Constr. Build. Mater. **274**, 122103 (2021). https://doi.org/10.1016/j.conbuildmat.2020.122103
14. V. Khoshsirat, H. Bayesteh, M. Sharifi, Effect of high salinity in grout on the performance of cement-stabilized marine clay, Constr. Build. Mater. **217**, 93–107 (2019). https://doi.org/10.1016/j.conbuildmat.2019.05.038
15. B. Shu, W. Chen, T. Yang, Z. Xie, Y. Ren, Y. Li, L. Zheng, G. Zeng, M. Li, D.M. Barbieri, Study on laboratory and engineering application of multi source solid waste based soft soil solidification materials, Case Stud. Constr. Mater. **17**, e01465 (2022). https://doi.org/10.1016/j.cscm.2022.e01465
16. A. Arulrajah, M. Yaghoubi, M.M. Disfani, S. Horpibulsuk, M.W. Bo, M. Leong, Evaluation of fly ash- and slag-based geopolymers for the improvement of a soft marine clay by deep soil mixing, Soils Found. **58**, 1358–1370, (2018). https://doi.org/10.1016/j.sandf.2018.07.005
17. S.D. Khadka, P.W. Jayawickrama, S. Senadheera, B. Segvic, Stabilization of highly expansive soils containing sulfate using metakaolin and fly ash based geopolymer modified with lime and gypsum, Transp. Geotech. **23**, 100327 (2020). https://doi.org/10.1016/j.trgeo.2020.100327
18. S. Kumar, R. Kumar, S.P. Mehrotra, Influence of granulated blast furnace slag on the reaction, structure and properties of fly ash based geopolymer, J. Mater. Sci. **45**, 607–615 (2010). https://doi.org/10.1007/s10853-009-3934-5
19. N.A. Odeh, A.H.J. Al-Rkaby, Strength, Durability, and Microstructures characterization of sustainable geopolymer improved clayey soil, Case Stud. Constr. Mater. **16**, e00988 (2022). https://doi.org/10.1016/j.cscm.2022.e00988
20. J.L. Provis, J.S.J. Deventer, Alkali Activated Materials State-of-the-Art Report, RILEM TC 224-AAM, Springer Dordrecht (2014). https://doi.org/10.1007/978-94-007-7672-2
21. C. Teerawattanasuk, P. Voottipruex, Comparison between cement and fly ash geopolymer for stabilized marginal lateritic soil as road material, Int. J. Pavement Eng. **20**, 1264–1274 (2019). https://doi.org/10.1080/10298436.2017.1402593
22. Q. Liu, Z. Chen, Z.M. El-Bahy, P. Wang, S.N. Abdou, M.M. Ibrahim, Y. Wan, J. Wang, H. Li, L. Li, H. Wang, Alkali-hydrothermal activation of tailings with red mud as a supplementary alkali source to synthesize one-part geopolymer, Adv. Compos. Hybrid Mater. 6 (2023). https://doi.org/10.1007/s42114-023-00707-3
23. ASTM C618, Standard Specification for Coal Fly Ash and Raw or Calcined Natural Pozzolan for Use in Concrete, USA (2022).
24. H. Yu, Y. Yi, K. Yao, A. Romagnoli, W.L. Tan, A.B.P. Chang, Effect of water/cement ratio on properties of cement-stabilized Singapore soft marine clay for wet deep mixing application, Int. J. Geotech. Eng. **15**, 1198–1205 (2021). https://doi.org/10.1080/19386362.2021.1890939
25. ASTM D6910/D6910M, Standard Test Method for Marsh Funnel Viscosity of Construction Slurries (2019).
26. ASTM C940, Standard Test Method for Expansion and Bleeding of Freshly Mixed Grouts for Preplaced-Aggregate Concrete in the Laboratory (2016).
27. ASTM D4972, Standard Test Methods for pH of Soils, (2019).
28. J.A. Cornell, Experiments with Mixtures: Designs, Models, and the Analysis of Mixture Data, Wiley (2011).
29. C. Suksiripattanapong, R. Sakdinakorn, S. Tiyasangthong, N. Wonglakorn, C. Phetchuay, W. Tabyang, Properties of soft Bangkok clay stabilized with cement and fly ash geopolymer for deep mixing application, Case Stud. Constr. Mater. 16 (2022). https://doi.org/10.1016/j.cscm.2022.e01081
30. X. Zhang, H. Zhu, Z. Jiao, Z. Cen, Lattice-shaped ground improvement by mixing soil and alkali-activated slag for liquefaction mitigation, Case Stud. Constr. Mater. **17**, e01445 (2022). https://doi.org/10.1016/j.cscm.2022.e01445
31. G. Mounika, U. Ramakrishna, G. Naresh Kumar Reddy, K. Suresh Kumar, A review on effect of red mud on properties of alkali activated materials (AAMs) and geopolymers (GPs), Mater. Today Proc. (2023). https://doi.org/10.1016/j.matpr.2023.03.446
32. M.E.C. Bruce, R.R. Berg, G.M. Filz, M. Terashi, D.S. Yang, J.G. Collin, S. Geotechnica, Federal Highway Administration design manual: Deep mixing for embankment and foundation support, United States. Federal Highway Administation (2013).
33. FDOT, Standard specifications for road and bridge construction (2025). https://www.fdot.gov.
34. A. Ward, Wireless In-Situ Slurry Testing Device, University of South Florida, USA (2025). https://digitalcommons.usf.edu/etd/11019
35. CETCO, Use of Shore Pac Polymer slurry: In slurry-displaced foundation construction (2022).
36. A.J. Puppala, R.S. Madhyannapu, S. Nazarian, D. Yuan, L. Hoyos, Deep Soil Mixing (DSM) Technology for Mitigation of Pavement Roughness, Texas Department of Transportation, USA, **7**, 100–104 (2008). http://tti.tamu.edu/documents/0-5179-1.pdf
37. G. Huang, X. Zhang, M. Liu, B. Fang, C. Wang, Compatibility of sodium hydroxide, sodium silicate and calcium-enriched additives in alkali-activated materials : From the perspectives of flowability , strength and microstructure, Constr. Build. Mater. **403** 133102 (2023). https://doi.org/10.1016/j.conbuildmat.2023.133102